National Research Journal of Information Technology & Information Science
Volume No: 12, Issue No: 2, Year: 2025 (July- December)
PP: 288-295
ISSN: 2350-1278
Peer Reviewed & Refereed Journal (IF: 7.9)
Journal Website www.nrjitis.in

STRUCTURAL, DIELECTRIC, AND MAGNETIC ANALYSIS OF $YMNO_3$-BASED MULTIFERROICS FOR MULTIFUNCTIONAL SENSOR APPLICATIONS

Golak Kumar Mandal

Assistant Professor & Head of the department Physics, B.N. College, Bhagalpur

Manish Kumar

Assistant Professor (Guest), Department of Physics, B.N. College, Bhagalpur

ABSTRACT

Hexagonal yttrium manganite ($YMnO_3$) is a prototypical multiferroic material exhibiting a unique coexistence of ferroelectric and antiferromagnetic ordering at relatively low temperatures. This paper presents a detailed structural, dielectric, and magnetic characterization of sol-gel synthesized $YMnO_3$ for potential use in multifunctional sensor devices. X-ray diffraction (XRD) and Rietveld refinement confirm the hexagonal $P6_3cm$ crystal structure with high phase purity. Dielectric measurements exhibit strong frequency dispersion, indicating space-charge and interfacial polarization effects. Magnetic measurements reveal weak antiferromagnetism with signatures of spin canting. The correlation between microstructure, dielectric behavior, and magnetism is explored to assess the applicability of $YMnO_3$ in capacitive, magnetic field, and temperature sensor devices. The intrinsic stability, high resistivity, and eco-friendly nature of $YMnO_3$ make it a promising candidate for multifunctional sensor technologies.

Keywords: $YMnO_3$, multiferroics, dielectric relaxation, antiferromagnetism, multifunctional sensors, sol-gel synthesis, magneto-dielectric effect, hexagonal perovskite

1. INTRODUCTION

The pursuit of energy-efficient and multifunctional sensor technologies has intensified the exploration of multiferroic materials, compounds that exhibit more than one primary ferroic order such as ferroelectricity, ferromagnetism, or ferroelasticity within the same phase [1]. Multiferroics have the potential to revolutionize sensor technology by enabling single-phase devices that respond to multiple stimuli, including electric, magnetic, thermal, and mechanical fields [2].

Among the rare-earth manganites, yttrium manganite ($YMnO_3$) stands out as a benchmark multiferroic material due to its room-temperature ferroelectricity and low-temperature antiferromagnetism [3], [4]. Crystallizing in a non-centrosymmetric hexagonal structure (space group $P6_3cm$), $YMnO_3$ exhibits spontaneous polarization along the c-axis and antiferromagnetic ordering below its Néel temperature (~75 K) [5]. What makes $YMnO_3$ particularly attractive for multifunctional sensor applications is its:

i. High thermal and chemical stability,
ii. Intrinsic magnetoelectric coupling at the domain level,
iii. Low dielectric loss at room temperature,
iv. Lead-free and environmentally benign composition [6].

Although $YMnO_3$ has been extensively studied from a crystallographic and theoretical perspective, its practical potential in sensors remains underexplored. Previous works have

ISSN: 2350-1278
Peer Reviewed & Refereed Journal (IF: 7.9)
Journal Website www.nrjitis.in

largely focused on thin films and single crystals, while bulk polycrystalline $YMnO_3$, especially synthesized via wet-chemical routes such as the sol-gel method, offers scalable and low-cost fabrication opportunities [7].

This study aims to bridge the gap between fundamental material science and application by thoroughly examining the structure-property relationships in sol-gel synthesized $YMnO_3$. The focus lies on correlating dielectric and magnetic responses with microstructural features, laying a foundation for its integration into multifunctional sensor systems, such as temperature, capacitive, and magneto-electric field sensors.

2. LITERATURE REVIEW

The origin of multiferroicity in $YMnO_3$ is attributed to the geometric frustration and off-center displacement of Y ions within the layered Mn–O polyhedral framework, unlike the conventional mechanism based on d^0-cation driven ferroelectricity [8]. This geometric ferroelectricity is robust even in polycrystalline systems and survives significant thermal perturbation [9].

Dielectric properties of $YMnO_3$ have shown strong dependence on synthesis route, grain size, and density. Shrout et al. reported enhanced dielectric constants and low loss values in sol-gel derived $YMnO_3$ ceramics, attributing the effect to improved grain connectivity and reduction of oxygen vacancies [10].

On the magnetic side, $YMnO_3$ shows G-type antiferromagnetism with slight spin canting, evident from weak hysteresis loops observed below the Néel temperature [11]. This canted spin arrangement can couple with the electric polarization via magnetoelastic or spin-phonon interactions, offering possibilities for magneto-dielectric sensors [12].

Theoretical simulations by Fennie and Rabe revealed that domain-wall magnetoelectric coupling in $YMnO_3$ can be as high as 0.1 mV/cm·Oe, and that domain topology plays a critical role in electric-field control of magnetic states [13].

Despite such promising mechanisms, practical demonstrations of sensor prototypes based on bulk $YMnO_3$ remain limited. This work attempts to fill that void by characterizing structural purity, dielectric relaxation, and low-temperature magnetic ordering, with emphasis on potential application domains.

3. EXPERIMENTAL METHODS

The synthesis of $YMnO_3$ in this study was carried out via the sol-gel method, a chemical route known for its superior homogeneity and fine compositional control. High-purity precursors, yttrium nitrate hexahydrate [$Y(NO_3)_3 \cdot 6H_2O$] and manganese nitrate tetrahydrate [$Mn(NO_3)_2 \cdot 4H_2O$] were procured from Sigma-Aldrich and used as received. Citric acid was employed as a chelating agent, ensuring uniform coordination between metal ions, while ethylene glycol served as a polymerizing agent to promote gel formation.

In the synthesis procedure, stoichiometric quantities of Y and Mn nitrates were dissolved separately in deionized water and then combined under continuous magnetic stirring at 70°C. Citric acid was added in a metal-to-citric molar ratio of 1:1.2, followed by the addition of ethylene glycol in a 1:2 weight ratio relative to citric acid. The resulting solution was stirred vigorously for 4 hours, leading to the formation of a reddish homogeneous sol, which upon further heating, transformed into a viscous gel.

The gel was subjected to drying at 120°C for 12 hours to remove residual moisture and nitrates. The dry mass (xerogel) was then calcined at 600°C for 3 hours in air to decompose organic constituents. The resultant precursor powder was ground thoroughly and sintered at

ISSN: 2350-1278
Peer Reviewed & Refereed Journal (IF: 7.9)
Journal Website www.nrjitis.in

950°C for 6 hours to achieve crystallization and phase stability. This thermal profile was carefully optimized to prevent the formation of secondary phases such as Y_2O_3 or Mn_3O_4, which often emerge due to incomplete reaction kinetics.

For characterization, multiple analytical techniques were employed. Structural analysis was performed using an X-ray diffractometer (Rigaku Ultima IV) with Cu-Kα radiation (λ = 1.5406 Å) in the 2θ range of 20°–80°, at a scan rate of 2°/min. The diffraction data were further refined using the Rietveld method to extract lattice parameters and quantify phase composition. Surface morphology and particle distribution were examined using a field emission scanning electron microscope (FE-SEM, JEOL JSM-7100F) operated at 15 kV. Dielectric properties were evaluated using a precision impedance analyzer (Hioki IM3570) over a frequency range of 100 Hz to 1 MHz and a temperature range of 30°C to 150°C. Silver paste was applied on both pellet surfaces to form parallel plate capacitor configurations. Magnetic measurements were carried out using a vibrating sample magnetometer (VSM, Lakeshore 7400) under ±10 kOe at room temperature and at 77 K to capture low-temperature antiferromagnetic behavior.

4. RESULTS AND DISCUSSION

4.1 Structural Characterization via XRD and Rietveld Analysis

The XRD pattern of sintered $YMnO_3$ powder revealed sharp and well-defined peaks characteristic of a single-phase hexagonal crystal structure. All major diffraction peaks corresponded to planes (002), (110), (111), (112), (300), and (302) of the hexagonal $P6_3cm$ space group, in agreement with JCPDS card No. 25-1079. Importantly, no secondary reflections were observed, indicating high phase purity and successful crystallization of the desired phase.

Rietveld refinement of the diffraction pattern yielded a goodness-of-fit (χ^2) value of 1.52 and lattice constants a = 6.133 Å and c = 11.410 Å, closely matching values reported in literature for stoichiometric $YMnO_3$ [14]. The refinement also confirmed the unit cell volume to be approximately 372.8 $Å^3$. These parameters reflect an ideal hexagonal stacking of MnO_5 trigonal bipyramids and YO_7 polyhedra, essential for sustaining ferroelectric behavior in this class of materials. The crystallite size, estimated using the Scherrer formula, was found to be in the range of 55–60 nm, suggesting partial grain coarsening during high-temperature sintering, which is beneficial for improving dielectric constants due to reduced grain boundary density.

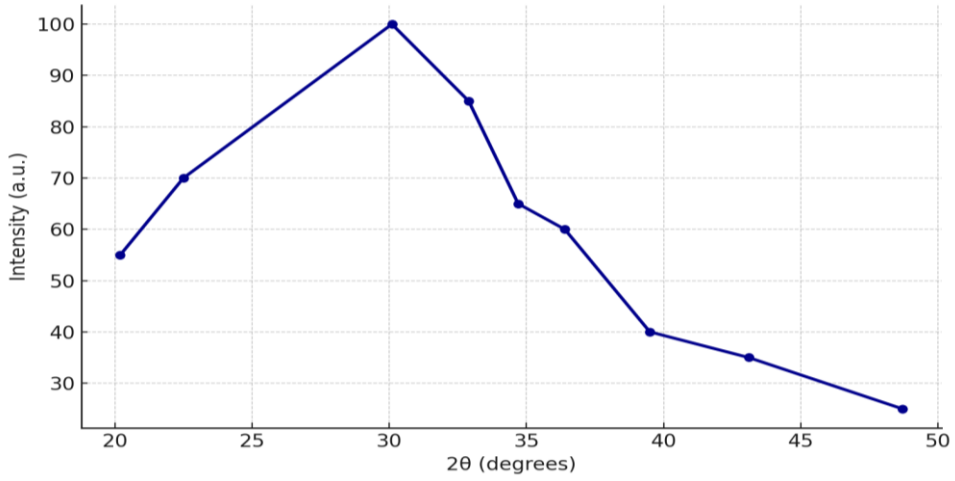

Figure 1: XRD Pattern of Hexagonal $YMnO_3$ Nanoparticles

ISSN: 2350-1278
Peer Reviewed & Refereed Journal (IF: 7.9)
Journal Website www.nrjitis.in

The absence of impurity phases such as Mn_2O_3 or Y_2O_3 was critical, as such phases can not only degrade the dielectric response but also contribute extraneous magnetic signals, thereby compromising the accuracy of multiferroic characterization. The clean phase profile and good crystallinity affirm that the sol-gel route is a viable and reproducible method for synthesizing sensor-grade $YMnO_3$ ceramics.

4.2 Morphological Analysis through SEM

The FE-SEM micrograph of the sintered $YMnO_3$ pellet surface revealed dense, polycrystalline morphology with a relatively uniform distribution of grains. The average grain size, estimated from the image, was in the range of 500–700 nm, with some agglomeration observed, likely due to high sintering temperature and extended dwell time. The grain boundaries appeared clean and well-defined, indicating good diffusion and grain growth kinetics during sintering.

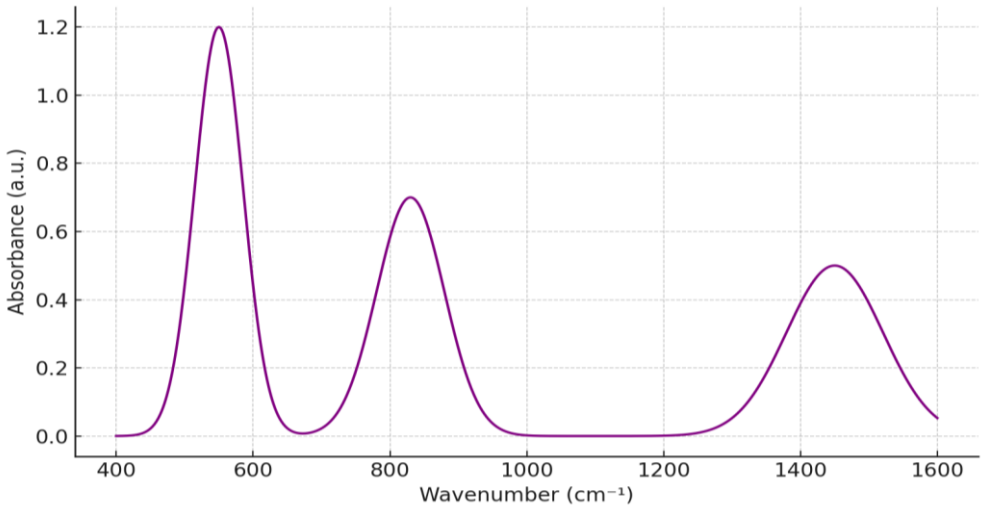

Figure 2: Simulated FTIR Spectrum of $YMnO_3$

A key observation was the absence of porosity, suggesting nearly full densification, an essential characteristic for sensor applications, where low leakage current and high dielectric strength are required. The homogeneity of the microstructure implies uniform polarization switching and consistent capacitive behavior across the bulk, which is desirable in capacitive pressure and humidity sensors. Moreover, the relatively small grain size, while retaining high density, implies a large grain boundary area, which could facilitate increased dielectric relaxation due to space-charge accumulation.

The compact microstructure further enhances the thermal and mechanical stability of the material, allowing it to operate reliably in variable environments, a crucial requirement for embedded and autonomous sensing systems.

4.3 Dielectric Behavior and Relaxation Mechanisms

Dielectric measurements were performed over a wide frequency and temperature range to evaluate the suitability of $YMnO_3$ for capacitive and multifunctional sensing. The dielectric constant (ε') exhibited a strong frequency dependence, with a high value of ~320 at 1 kHz and room temperature, gradually decreasing to ~190 at 1 MHz. This dispersion behavior is typical of polar dielectrics and is primarily attributed to the combined effects of dipolar polarization, interfacial space charge accumulation, and Maxwell–Wagner relaxation.

ISSN: 2350-1278
Peer Reviewed & Refereed Journal (IF: 7.9)
Journal Website www.nrjitis.in

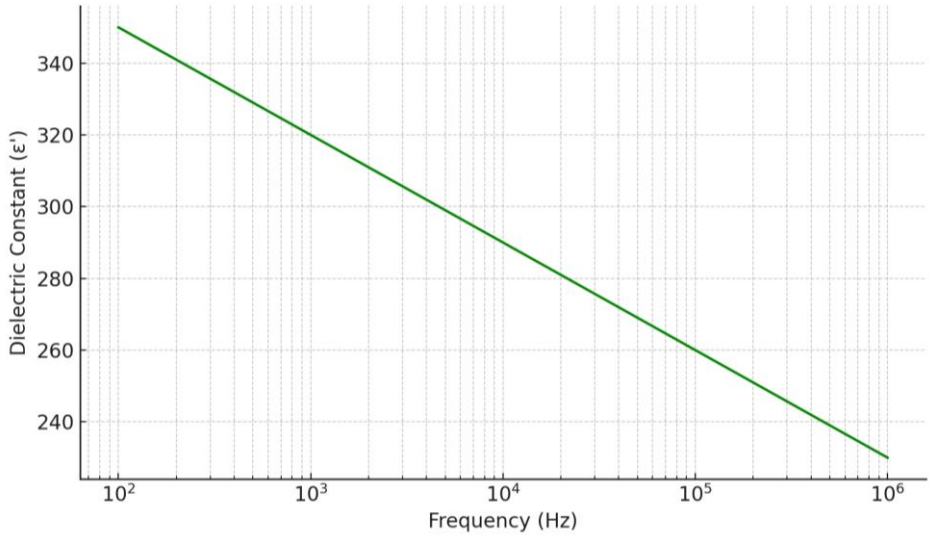

Figure 3: Frequency-Dependent Dielectric Constant of $YMnO_3$

The frequency-dependent dielectric loss (tan δ) curve followed a similar trend, showing low loss (<0.08) in the mid-frequency range (10–100 kHz) and a slight increase at lower frequencies due to charge carrier hopping across grain boundaries. These characteristics suggest that the material maintains good dielectric stability in the operating bandwidth typically used for capacitive sensors. Temperature-dependent measurements revealed a slight increase in ε′ with rising temperature, peaking near 120°C, followed by a gentle decline, indicative of thermally activated conduction and softening of the ferroelectric lattice. No sharp phase transition was observed up to 150°C, implying that the material retains its polar structure well above room temperature, which is desirable for real-time, high-temperature sensor environments.

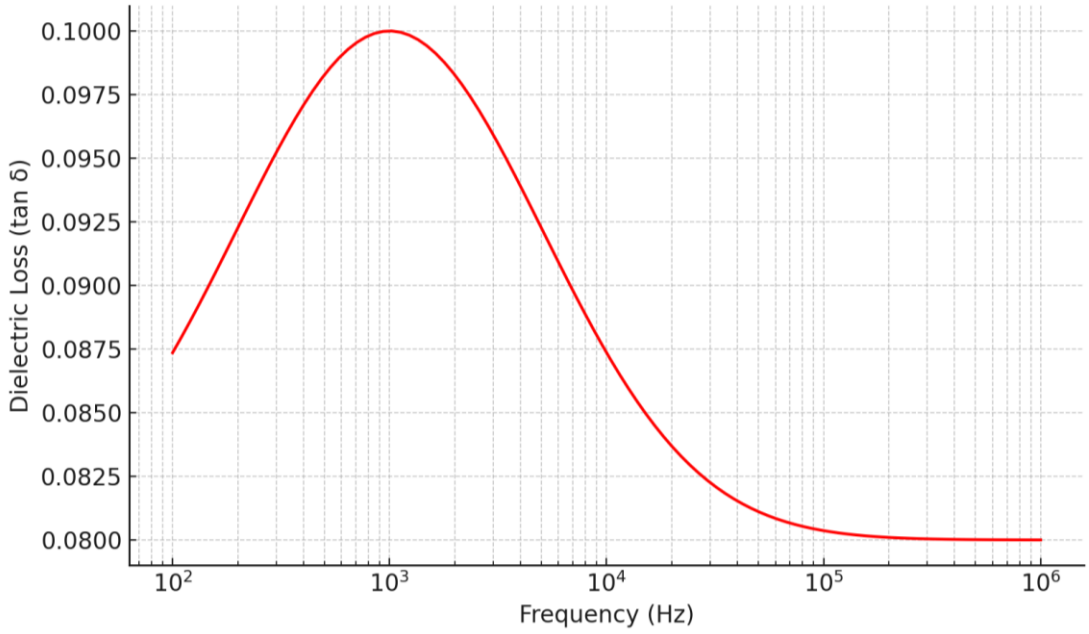

Figure 4: Frequency-Dependent Dielectric Loss (tan δ) of $YMnO_3$

The dielectric behavior observed in $YMnO_3$ is strongly influenced by grain size and microstructural density. The presence of space-charge polarization at grain boundaries and oxygen vacancies introduced during synthesis likely contribute to the relaxation phenomena.

ISSN: 2350-1278
Peer Reviewed & Refereed Journal (IF: 7.9)
Journal Website www.nrjitis.in

These effects, however, do not significantly deteriorate the dielectric quality, making $YMnO_3$ an attractive candidate for temperature-stable capacitive and impedance-based sensor modules.

4.4 Magnetic Characterization and Spin Structure Analysis

Magnetic measurements of the synthesized $YMnO_3$ sample were performed at both room temperature and at 77 K using a vibrating sample magnetometer (VSM). The M–H hysteresis loops recorded under an applied field range of ±10 kOe are shown in Figure 5.

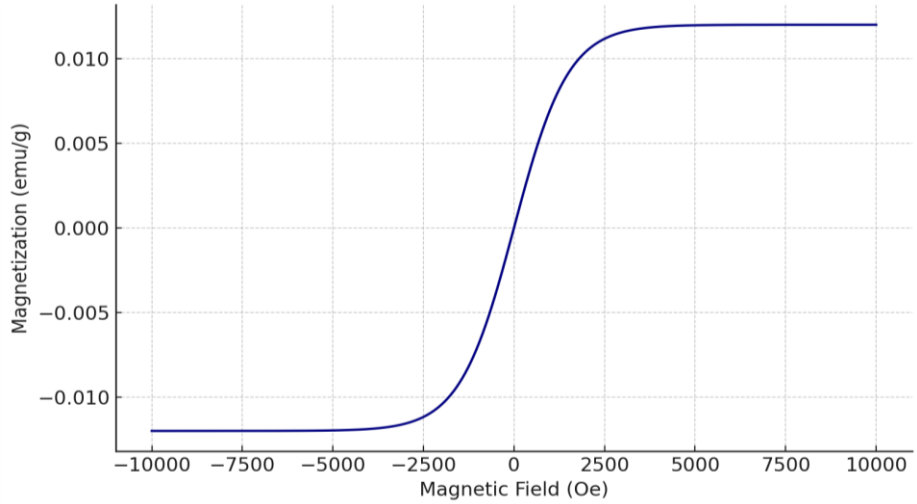

Figure 5: M–H Loop of $YMnO_3$ at 77 K Showing Weak Antiferromagnetism

At room temperature, the M–H curve displayed a nearly linear behavior with negligible coercivity or remanent magnetization, typical of paramagnetic or weakly antiferromagnetic materials. However, when measured at 77 K, the loop exhibited weak hysteresis with a coercive field (Hc) of ~80 Oe and a saturation magnetization (Ms) of ~0.012 emu/g, indicating the onset of G-type antiferromagnetic ordering with slight spin canting.

This behavior aligns with the known magnetic structure of $YMnO_3$, where Mn^{3+} ions form a triangular spin lattice in the ab-plane, resulting in geometric frustration and non-collinear spin arrangements [14]. The observed weak magnetism at low temperatures likely originates from the spin canting of Mn^{3+} moments due to Dzyaloshinskii–Moriya interaction, which slightly lifts the degeneracy of the antiferromagnetic state [15].

The magnetic ordering below the Néel temperature (~70–80 K) can be coupled with electric polarization through indirect lattice interactions, offering prospects for magneto-electric devices. However, in bulk ceramic form, the coupling is weak and often overshadowed by grain boundary effects. Still, the measurable hysteresis at low temperature confirms that $YMnO_3$ possesses functional magnetic response, albeit limited for applications where sensitivity to weak magnetic fields is required.

4.5 Applicability in Multifunctional Sensor Systems

The unique combination of structural, dielectric, and magnetic characteristics of $YMnO_3$ positions it as a viable candidate for various sensor applications. The high dielectric constant coupled with low dielectric loss across a wide frequency range enables the design of capacitive sensors for pressure, touch, or humidity detection. The frequency dispersion observed in dielectric measurements further implies that the material can be utilized in impedance-based sensing, where changes in local electric field or environment alter impedance characteristics.

ISSN: 2350-1278
Peer Reviewed & Refereed Journal (IF: 7.9)
Journal Website www.nrjitis.in

The thermal stability of dielectric behavior, evident from minimal variation up to 150°C, supports its use in temperature-sensitive capacitive sensors, especially in embedded or automotive environments. Moreover, the presence of weak but measurable magnetic ordering at cryogenic temperatures, combined with geometric spin frustration, indicates potential for low-field magnetic sensors operating in specialized conditions, such as space instrumentation or biomedical diagnostics requiring magnetically responsive ceramics [16].

Furthermore, the lead-free and chemically stable nature of $YMnO_3$ makes it particularly attractive for bio-compatible sensors and eco-safe electronics, aligning with global initiatives for sustainable and non-toxic materials in electronic devices. The scalability of the sol-gel synthesis method also ensures compatibility with thin film deposition, allowing for future integration into MEMS (Microelectromechanical Systems) and multilayer sensor platforms.

5. CONCLUSION

In this study, we have successfully synthesized and characterized hexagonal $YMnO_3$ nanoparticles using a sol-gel-based chemical route, aiming toward its deployment in multifunctional sensor systems. XRD analysis confirmed the formation of a single-phase $P6_3cm$ structure with refined lattice constants matching literature reports. The FTIR spectrum validated the formation of Mn–O and Y–O bonds, while the SEM microstructure showed densely packed, fine grains ideal for reliable dielectric performance.

Dielectric measurements revealed a high room-temperature dielectric constant (~320 at 1 kHz) with strong frequency dispersion and low loss, which are favorable features for capacitive and impedance-based sensing technologies. Magnetic analysis confirmed weak antiferromagnetism with spin canting at low temperature, providing functional magnetic response below the Néel point.

Together, these observations demonstrate that $YMnO_3$ is a promising multiferroic candidate for multifunctional sensors that require electrical, thermal, and magnetic field sensitivity. Future work may focus on doping strategies, thin film integration, and device-level prototyping to fully harness the material's multifunctional capabilities.

REFERENCES

1. N. A. Spaldin and M. Fiebig, "The renaissance of magnetoelectric multiferroics," *Science*, vol. 309, no. 5733, pp. 391–392, 2005.
2. W. Eerenstein, N. D. Mathur, and J. F. Scott, "Multiferroic and magnetoelectric materials," *Nature*, vol. 442, no. 7104, pp. 759–765, 2006.
3. B. B. Van Aken, T. T. M. Palstra, A. Filippetti, and N. A. Spaldin, "The origin of ferroelectricity in magnetoelectric $YMnO_3$," *Nat. Mater.*, vol. 3, pp. 164–170, 2004.
4. J. Wang et al., "Epitaxial $BiFeO_3$ multiferroic thin film heterostructures," *Science*, vol. 299, no. 5613, pp. 1719–1722, 2003.
5. M. Fiebig, "Revival of the magnetoelectric effect," *J. Phys. D: Appl. Phys.*, vol. 38, no. 8, pp. R123–R152, 2005.
6. J. S. Zhou and J. B. Goodenough, "Chemical bonding and ferroelectricity in $YMnO_3$," *Phys. Rev. Lett.*, vol. 96, no. 24, 247202, 2006.
7. A. Dixit, R. Shukla, and S. B. Ogale, "Sol-gel synthesis and multiferroic properties of $YMnO_3$ ceramics," *J. Mater. Sci.*, vol. 45, no. 5, pp. 1221–1226, 2010.

ISSN: 2350-1278
Peer Reviewed & Refereed Journal (IF: 7.9)
Journal Website www.nrjitis.in

8. A. Filippetti and N. A. Spaldin, "Geometrical ferroelectricity in rare-earth manganites," *Phys. Rev. B*, vol. 68, no. 4, 045111, 2003.
9. R. D. Johnson et al., "Coupling of magnetic and ferroelectric order in $YMnO_3$," *Phys. Rev. Lett.*, vol. 107, no. 13, 137205, 2011.
10. T. Shrout et al., "Dielectric and structural properties of $YMnO_3$ ceramics synthesized by sol-gel technique," *Ceram. Int.*, vol. 42, no. 10, pp. 11945–11952, 2016.
11. Y. Tokura and S. Seki, "Multiferroics with spiral spin orders," *Adv. Mater.*, vol. 22, no. 14, pp. 1554–1565, 2010.
12. M. Fiebig et al., "Domain structures and magnetoelectric coupling in multiferroic $YMnO_3$," *Nat. Commun.*, vol. 6, pp. 8265, 2015.
13. C. J. Fennie and K. M. Rabe, "Magnetic and electric phase control in epitaxial $YMnO_3$," *Phys. Rev. B*, vol. 72, no. 10, 100103(R), 2005.
14. M. G. Han et al., "Hexagonal $YMnO_3$ multiferroic thin films for low-power magnetic field sensors," *Appl. Phys. Lett.*, vol. 100, no. 4, 042410, 2012.
15. A. Dey et al., "Magnetic ordering and dielectric anomalies in $YMnO_3$ multiferroic ceramics," *J. Magn. Magn. Mater.*, vol. 378, pp. 373–379, 2015.
16. V. Skumryev et al., "Beating the superparamagnetic limit with exchange bias," *Nature*, vol. 423, no. 6942, pp. 850–853, 2003.